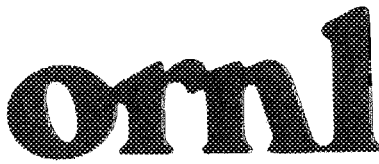




3 4456 0330575 0

ORNL/TM-11705



**OAK RIDGE  
NATIONAL  
LABORATORY**

**MARTIN MARIETTA**

**Technical Background for  
Shallow (Skin) Dose  
Equivalent Evaluations**

J. C. Ashley  
J. E. Turner  
O. H. Crawford  
R. N. Hamm  
K. L. Reaves  
K. L. McMahan

OAK RIDGE NATIONAL LABORATORY  
CENTRAL RESEARCH LIBRARY  
CIRCULATION SECTION  
4509 ROAD 175  
**LIBRARY LOAN COPY**  
DO NOT TRANSFER TO ANOTHER PERSON  
If you wish someone else to see this  
report, send in name with report and  
the library will arrange a loan.

MANAGED BY  
MARTIN MARIETTA ENERGY SYSTEMS, INC.  
FOR THE UNITED STATES  
DEPARTMENT OF ENERGY

This report was prepared as an essential part of the work of the following agency:

Executive Order 11652, 1972, provided for the development of a new type of letter call letterhead. P.L. 92-501, October 1972, provided for the development of (S-15) 576 and (S-15) 576-2.

Available to the public through the National Technical Information Service, U.S. Department of Commerce, 5285 Port of Spain, Springfield, VA 22161.

This report was prepared as an essential part of work sponsored by an agency of the United States Government. Neither the United States Government nor any agency thereof, nor any of their employees, makes any warranty, expressed or implied, or assumes any legal liability or responsibility for the accuracy, completeness, or usefulness of any information, apparatus, product, or process disclosed, or represents that its use would not infringe privately owned rights. Reference herein to any specific commercial product, process, or service by trade name, trademark, manufacturer, or otherwise, is not necessarily constitutive or imply its endorsement, recommendation, or approval by the United States Government or any agency thereof. The views and opinions of authors expressed herein do not necessarily state or reflect those of the United States Government or any agency thereof.

ORNL/TM-11705

TECHNICAL BACKGROUND FOR SHALLOW  
(SKIN) DOSE EQUIVALENT EVALUATIONS

J. C. Ashley, J. E. Turner,  
Oakley H. Crawford, and R. N. Hamm  
Health and Safety Research Division

and

K. L. Reaves and K. L. McMahan  
Office of Environmental and Health Protection

Oak Ridge National Laboratory  
Post Office Box 2008  
Oak Ridge, TN 37831-6285

Date Published — January 1991

Prepared by the  
OAK RIDGE NATIONAL LABORATORY  
Oak Ridge, Tennessee 37831  
managed by  
MARTIN MARIETTA ENERGY SYSTEMS, INC.  
for the  
U.S. DEPARTMENT OF ENERGY  
under contract DE-AC05-84OR21400

MARTIN MARIETTA ENERGY SYSTEMS LIBRARIES



3 4456 0330575 0



## TABLE OF CONTENTS

I. Introduction . . . . .	1
II. Dose Rates from Skin Contamination. . . . .	1
III. Measurements with Calibrated Sources . . . . .	2
IV. Evaluation of Conversion Factors. . . . .	4
V. Some Approximations in Determining Conversion Factors . . . . .	6
References. . . . .	10
Table I. Summary of Measurements on Calibrated Sources . . . . .	11
Table II. Conversion Factors (Case A). . . . .	12
Table III. Conversion Factors (Case B) . . . . .	13
Table IV. Conversion Factors (Case C) . . . . .	14
Appendix A – Effects of the Tissue–Air Interface. . . . .	15
Appendix B – Solid–Angle (Geometrical) Factors . . . . .	36
Distribution List . . . . .	39



TECHNICAL BACKGROUND FOR SHALLOW  
(SKIN) DOSE EQUIVALENT EVALUATIONS

I. INTRODUCTION

Department of Energy Order 5480.11 [1] describes procedures for radiation protection for occupational workers. The revisions dealing with non-uniform exposure to the skin [Section 9.f.(2)] are the subject of this report. We describe measurements and analysis required to assess shallow (skin) dose equivalent from skin contamination.

II. DOSE RATES FROM SKIN CONTAMINATION

The shallow (skin) dose equivalent, or dose equivalent to the basal layer at a depth of 70  $\mu\text{m}$ , from radioactive contamination on the surface of the skin cannot be directly measured and must be inferred from calculations. The skin dose-equivalent rate  $\dot{H}(\text{rem/h})$  can be related to a uniform activity concentration  $C(\mu\text{Ci}/\text{cm}^2)$  on an infinite surface by writing

$$\dot{H} = C \times V,$$

where  $V[(\text{rem/h})/(\mu\text{Ci}/\text{cm}^2)] = V_{\beta} + V_{\gamma}$  is a conversion factor that contains contributions from both beta particles and gamma rays. Values of  $V_{\beta}$  have been calculated from the computer code VARSKIN and tabulated for several beta sources [2]. Results for  $V_{\beta}$  for a much more extensive list of isotopes, using a different method of calculation, have been tabulated by Kocher and Eckerman [3]. Good agreement is found for values of  $V_{\beta}$  between these two tabulations. These results

are becoming widely accepted as a basis for estimating shallow (skin) dose equivalent (see, e.g., Ref. 4). Recent work has shown that dose estimates may be influenced significantly by including a skin-air interface not considered in the "infinite medium" results in Refs. 2 and 3; studies of this effect are discussed in Appendix A (and references therein).

For non-uniform contamination over a finite area (including point sources), the computer code VARSKIN can be used to evaluate the dose rate, at points in the basal layer, or averaged over some given area in the basal layer. Note that VARSKIN gives the contributions from beta particles only. Contributions from gamma rays, if present, require a separate calculation; guidance for evaluating this contribution can be found in Refs. 2, 4, and 5. Usually the gamma component of the dose rate for skin contamination is relatively small ( $\lesssim 20\%$ ; see [4-5]).

While dose rate in the basal layer can be evaluated from a knowledge of the activity and area of contamination, for screening purposes we must use survey-meter readings to make an initial judgement of its magnitude. In the next section we describe a method for obtaining screening estimates of skin dose equivalent from count rates and times of exposure, based on available information on dose-rate conversion factors and experimental data for a specific probe and selected isotopes.

### III. MEASUREMENTS WITH CALIBRATED SOURCES

Measurements were made with BICRON pancake probe, Model PGM, and calibrated sources of  $^{99}\text{Tc}$ ,  $^{90}\text{Sr}/^{90}\text{Y}$ ,  $^{14}\text{C}$ ,  $^{36}\text{Cl}$ , and  $^{147}\text{Pm}$ . These disc sources had diameters of 2.54 cm or 4 cm. Count rates (counts per minute, cpm) were measured for four configurations: (A) source on the "face-up" probe, (B) probe 1 cm from the source, (C) probe 1 cm from the source with an intervening collimator with an

opening area 1 cm<sup>2</sup>, and (D) source on a surface covered with the "face-down" probe. Configurations (A) and (D) gave essentially the same count rates, and so Case D is not reported. The cpm measurements are given in Table I indicating the nuclide, source identification, maximum beta-particle energy, and data from the calibration sheets on active diameter and source strength. All the sources are pure beta emitters.

The activities of two of the sources had changed appreciably since the calibration date because of radioactive decay. If  $A_0$  is the activity at calibration and  $T$  is the half-life, then the activity in disintegrations per minute (dpm) at a time  $\Delta t$  after calibration is summarized as follows for the two sources:

<sup>147</sup>Pm:            Calibration date: October 13, 1988 ;  $A_0 = 0.250 \mu\text{Ci}$   
                           Measurement date: March 19, 1990  
 $\Delta t \approx 1 \text{ yr.}, 5 \text{ mo.} = 1.42 \text{ y}$  ;  $T = 2.62 \text{ y}$   
 $A = A_0 \exp(-0.693 \Delta t / T) = 0.1717 \mu\text{Ci}$   
 $\text{dpm} = 2.22 \times 10^6 A = 3.81 \times 10^5$

<sup>90</sup>Sr:                Calibration date: December 19, 1988 ;  $A_0(\text{Sr}) = 0.030 \mu\text{Ci}$   
                           Measurement date: March 19, 1990  
 $\Delta t = 1 \text{ yr.}, 3 \text{ mo.} = 1.25 \text{ y}$  ;  $T = 28.5 \text{ y}$   
 $A = A_0 \exp(-0.693 \Delta t / T) = 0.02910 \mu\text{Ci}$   
 $\text{dpm} = 2.22 \times 10^6 A = 6.46 \times 10^4$   
 For each <sup>90</sup>Sr decay, a short-lived ( $T = 2.67 \text{ d}$ ) daughter, <sup>90</sup>Y,  
 is produced which decays by  $\beta$  emission.

#### IV. EVALUATION OF CONVERSION FACTORS

In Table II we give the net count rate for source—detector configuration (A) and the derived "efficiency" cpm/dpm. The factor V in Table II connects the shallow (skin) dose equivalent, H(70), the dose equivalent at a depth of 70  $\mu\text{m}$ , to the source activity. Table 3.1, Ref. 2, gives dose—rate factors V ( $= V_{\beta}$ ) in  $[(\text{rem/h})/(\mu\text{Ci}/\text{cm}^2)]$  calculated from the computer code VARSKIN for a number of  $\beta$  emitters. We note that these dose—rate factors are in good agreement with those calculated by Kocher and Eckerman [3]. Reference 3 presents a much more extensive list of nuclides than Ref. 2.

Regulations [1] specify that 1  $\text{cm}^2$  is the smallest area over which the shallow (skin) dose equivalent is to be averaged. The calculations described in Appendix A show that, for a given amount of activity, average dose equivalent over 1  $\text{cm}^2$  is independent of the area occupied by the source up to 1  $\text{cm}^2$ . To be conservative in determining the conversion factor, CF, we assume the activity "observed" by the detector came from 1  $\text{cm}^2$ . We thus obtain the conversion factors in Table II which should give reasonable and conservative estimates of shallow (skin) dose equivalents directly from measured cpm.

Generally, the detection efficiency (cpm/dpm) of G—M detectors is low for pure  $\beta$  emitters with low maximum  $\beta$ —particle energies, as illustrated in Table II. The dose—rate factors also tend to be smaller for nuclides with lower maximum  $\beta$  energies. The conversion factors CF in the last column in Table II, which contain ratios of the above two quantities, show much less variation over a range of nuclides than the two quantities individually. Our values of CF fall in the range  $0.5\text{--}3 \times 10^{-5}$  (rem/h)/cpm with the lower—energy nuclides having lower values. Similar compensation and clustering of values around  $2 \times 10^{-5}$  (rem/h)/cpm has been described by Flood [4]. With the probe in contact with the source, we recommend

the value  $CF = 5 \times 10^{-5}$  (rem/h)/cpm for preliminary screening of contamination incidents with a known or unknown  $\beta$  source.

Measurement set (B), Table I, was made with the source disc parallel to the detector face at a separation of 1 cm. If we assume the source activity is concentrated in a disc of area 1 cm<sup>2</sup> (disc radius 0.564 cm) instead of its original area (radius  $r_s$ ) the measured (cpm)<sub>o</sub> will be modified by geometrical factors, G, to

$$(cpm)' = (cpm)_o G(0.564, 2.22) / G(r_s, 2.22). \quad (1)$$

$G(r_s, r_D)$  corresponds to a source disc of radius  $r_s$  centered 1 cm below, and parallel to, the detector face of radius  $r_D$ . The derivation of these factors and a table of values are given in Appendix B. The results from measurement set (B), modified according to Eq. (1), are given in Table III. For this probe-source configuration, a conservative value of  $CF = 1 \times 10^{-4}$  (rem/h)/cpm can be used for screening purposes or for an unknown  $\beta$  source.

Measurement set (C) corresponds to cpm using a collimator designed to measure 1 cm<sup>2</sup> of the source with the detector separated from the source by 1 cm. For the calculations of CF for this situation we assume the activity on the source disc is distributed uniformly and the detector "sees" only 1 cm<sup>2</sup> of the disc. The results of these calculations are given in Table IV. Measurements with such a collimator may be used to help define the area of contamination or to obtain "on-scale" readings from areas of high activity. For this configuration, a conservative value of  $CF = 3 \times 10^{-4}$  (rad/h)/cpm can be used for screening purposes or for an unknown  $\beta$  source.

## V. SOME APPROXIMATIONS IN DETERMINING CONVERSION FACTORS

The nuclides used in the measurements given in Table I were mounted on stainless steel (or nickel) backings. The  $^{99}\text{Tc}$  sources have no covering layer while the other sources are said to be covered with a mylar window of thickness  $0.9 \text{ mg/cm}^2$  (and not a number 100 times larger shown on the calibration certificates). Here we estimate the influence of backscattering and covers on the dose-equivalent conversion factors (CF) given in Tables II, III, and IV, and on resulting values of shallow (skin) dose equivalent. The possible effect of self-absorption in the sources is discussed qualitatively.

### Backscattering

Assume a radioactive material which produces  $\beta$ 's at a rate dpm is spread on an air-solid interface. Neglect backscattering from air and let  $\eta$  be the fraction of the  $\beta$ 's that move initially into the solid and are scattered back into air. For an isotropic distribution the number of  $\beta$ 's directed into the air is  $(\text{dpm}) \cdot (2\pi/4\pi) \cdot (1 + \eta)$ . For a fixed geometry with the assumption that the backscattered  $\beta$ 's are as likely to be counted as those initially directed into air, the count rate from a detector outside the surface is related to the count rate in the absence of backscattering  $(\text{cpm})_o$ , by

$$\text{cpm} = (\text{cpm})_o (1 + \eta) .$$

In the Tables, cpm is for stainless steel (ss) or nickel while the field measurements of cpm will be for skin. These are related by

$$(\text{cpm})_{\text{ss}} = \frac{(1 + \eta_{\text{ss}})}{(1 + \eta_{\text{skin}})} (\text{cpm})_{\text{skin}}$$

Since the dose-equivalent conversion factors are inversely proportional to cpm, the  $\text{CF}_{\text{ss}}$  in the tables are related to those for skin by

$$\text{CF}_{\text{ss}} = \frac{(1 + \eta_{\text{skin}})}{(1 + \eta_{\text{ss}})} \text{CF}_{\text{skin}}$$

For  $\eta_{\text{ss}} = 0.25$  (as assumed for the source calibrations),  $\text{CF}_{\text{ss}} = (4/5)(1 + \eta_{\text{skin}})$ , and the Table values underestimate those for skin by up to 25% (for  $\eta_{\text{skin}} = 0$ ). If  $\eta_{\text{skin}} = .05$ ,  $\text{CF}_{\text{ss}} = 0.84 \text{CF}_{\text{skin}}$  and  $\text{CF}_{\text{ss}}$  would underestimate  $\text{CF}_{\text{skin}}$  by  $\approx 20\%$ .

Estimates of shallow (skin) dose equivalent are to be obtained from measurements of  $(\text{cpm})_{\text{skin}}$  and residence time of the contamination on the skin. From the above discussion it appears that estimates of  $\text{H}(70)$  or  $\dot{\text{H}}(70)$  based on the table values of CF for specific nuclides will underestimate the true value by  $\lesssim 25\%$  due to backscattering.

### Source Covers

The disc sources listed in the Tables, except for  $^{99}\text{Tc}$ , have  $0.9 \text{ mg/cm}^2$  Mylar covers over the active layer. The main influence of the cover is to reduce the energy of the  $\beta$ 's passing through this layer on their way to the detector. This has the effect of shifting the spectrum to lower energies with the lower energies affected more than the higher energies, since the stopping power of Mylar decreases from  $6.15 \text{ MeV cm}^2/\text{g}$  at  $50 \text{ keV}$  to  $1.70 \text{ MeV cm}^2/\text{g}$  at  $1.5 \text{ MeV}$  [6]. For example, a  $50\text{-keV}$   $\beta$  will be reduced in energy by  $\sim 10\%$  on passing through the cover normal to the surface ( $\Delta E \approx 5.5 \text{ keV}$ ). Thus some of the  $\beta$ 's that might have been energetic enough to enter the detector will no longer be able to do so; a normally incident  $\beta$

must have an energy  $\gtrsim 45$  keV to "get through" the detector window. The presence of the cover on a disc source will thus reduce the measured cpm, compared with an uncovered source. This and the increased cpm for the "uncovered" nuclide as measured on the skin combine to provide an overestimate of the shallow (skin) dose equivalent using the CF numbers in the tables.

The size of this overestimate is expected to be small for  $\beta$  spectra with large average  $\beta$  energies,  $E_{\beta}^{AV}$  (e.g.,  $E_{\beta}^{AV} = 251$  keV for  $^{36}\text{Cl}$ ). However, for  $^{14}\text{C}$  ( $E_{\beta}^{AV} = 49$  keV) and  $^{147}\text{Pm}$  ( $E_{\beta}^{AV} = 62$  keV), cutting out part of the spectrum somewhere near the peak, and the resulting reduction in cpm, will be a larger effect.

The influence of the cover produces conservative estimates of shallow (skin) dose equivalent when the Table conversion factors for specific nuclides are used. If refined values for  $H(70)$  or  $\dot{H}(70)$  are considered essential, estimates of the size of this effect can be made.

#### Self-Absorption

The sources used in these measurements (other than  $^{99}\text{Tc}$ ) are described in the calibration sheets as follows.

"The activity is dispersed on a 40mm diameter qualitative filter paper, which is bonded to a stainless steel disc, covered with a 90 mg/cm<sup>2</sup> (sic) mylar window, and crimped into an aluminum mount."

The thickness of the Mylar window, apparently stated incorrectly in the above description, and its influence in the connection between dpm and measurements of cpm is discussed above. These sources are apparently formed by placing a given amount of solution containing the nuclide on filter paper and allowing the solvent to evaporate. No information was given on the thickness of the filter paper, but, as

argued below, self-absorption should lead to conservative estimates for dose-equivalent rates.

Assume that the nuclide is dispersed uniformly throughout the filter paper. If the filter paper is "thick" enough, the  $\beta$ 's seen outside the source, after some attenuation in the window, will have come from a "thin" top layer of the filter paper. The dpm stated for the source is for all the nuclide in the filter paper. Thus, in this situation, we expect fewer  $\beta$ 's to exit the source and be available for counting than predicted simply from the dpm. The ratio of measured cpm to stated dpm in the source will be smaller than for the same activity in a non-self-absorbing layer of the same area. This implies that the CF's in the tables are overestimates, since they include that ratio in the denominator. If the filter paper is thick enough so that self-absorption is important, then there will be no contribution to the cpm from backscatter on the substrate.

REFERENCES

1. DOE (Department of Energy), DOE Order 5480.11, "Radiation Protection for Occupational Workers," US-DOE, 12-21-88 + DRAFT CHANGES (3-5-90).
2. R. S. Traub, W. D. Reese, R. I. Scherpelz, and L. A. Sigalla, "Dose Calculation for Contamination of Skin Using the Computer Code VARSKIN," NUREG/CR-4418, PNL-5610, August 1987. Available from RSIC Computer Code Collection as CCC-522/VARSKIN.
3. D. C. Kocher and K. F. Eckerman, "Electron Dose-Rate Conversion Factors for External Exposure of the Skin from Uniformly Deposited Activity on the Body Surface," *Health Phys.* 53, 135-141 (1987).
4. John. R. Flood, "Practical Methods for Determining Dose from Radioactive Skin Contamination," *Radiation Protection Management* 5 (No. 3), 29-37 (1988).
5. Peter Murphy, "Calculating Gamma Dose Factors for Hot Particle Exposures," *Radiation Protection Management* 7, (No. 3), 38-42 (1990).
6. "Stopping Powers for Electrons and Positrons," ICRU Report 37 (International Commission on Radiation Units and Measurements, Bethesda, MD 20814, October, 1984).

TABLE I. SUMMARY OF MEASUREMENTS ON CALIBRATED SOURCES FOR THREE SOURCE-PROBE CONFIGURATIONS: A - SOURCE DISC IN CONTACT WITH PROBE FACE; B - SOURCE DISC CENTERED ON, PARALLEL TO, AND 1 CM FROM PROBE FACE; C - SOURCE DISC CENTERED ON 1 CM<sup>2</sup> CYLINDRICAL COLLIMATOR, 1 CM FROM PROBE FACE.

NUCLIDE	MAXIMUM BETA ENERGY (MeV)	T <sub>1/2</sub>	SERIAL NO. OF SOURCE	ACTIVE DIAMETER (cm)	dpm	COUNTS PER MINUTE (GROSS)†		
						A	B	C
<sup>99</sup> Tc	0.292	2.12x10 <sup>5</sup> y	1404/89	2.54	1.49x10 <sup>4</sup>	4034	2012	245
<sup>90</sup> Sr/ <sup>90</sup> Y	0.546/2.27	29.1y/2.67d	S9999098-18	4.0	6.46x10 <sup>4</sup> *	39091	20352	995
<sup>14</sup> C	0.156	5.73x10 <sup>3</sup> y	S9999098-10	4.0	7.77x10 <sup>5</sup>	12799	6039	291
<sup>36</sup> Cl	0.714	3.01x10 <sup>5</sup> y	S9999098-13	4.0	1.78x10 <sup>5</sup>	48778	28250	1323
<sup>147</sup> Pm	0.224	2.62y	S9999098-05	4.0	3.81x10 <sup>5</sup> *	18566	9811	431

\*Corrected for decay from calibration date to measurement date.

†Includes background of: 70 cpm (<sup>99</sup>Tc) and 53 cpm (others) for A and B; 62 cpm (<sup>99</sup>Tc) and 37 cpm (others) for C.

TABLE II. CONVERSION FACTORS FOR EVALUATING SHALLOW (SKIN) DOSE EQUIVALENT FROM COUNT-RATE MEASUREMENTS: CASE A - SOURCE DISC IN CONTACT WITH PROBE FACE.

NUCLIDE	dpm	cpm†	$\frac{\text{cpm}}{\text{dpm}}$	$V \left( \frac{\text{rem/h}}{\mu\text{Ci/cm}^2} \right)$	$CF \left( \frac{\text{rem/h}}{\text{cpm}} \right)$
<sup>99</sup> Tc	1.49x10 <sup>4</sup>	3964	0.266	3.49	5.91x10 <sup>-6</sup>
<sup>90</sup> Sr/ <sup>90</sup> Y	6.46x10 <sup>4</sup> *	39038	0.604	6.76/9.29	1.20x10 <sup>-5</sup>
<sup>14</sup> C	7.77x10 <sup>5</sup>	12746	0.0164	1.09	2.99x10 <sup>-5</sup>
<sup>36</sup> Cl	1.78x10 <sup>5</sup>	48725	0.274	7.44	1.22x10 <sup>-5</sup>
<sup>147</sup> Pm	3.81x10 <sup>5</sup> *	18513	0.0486	2.19	2.03x10 <sup>-5</sup>

\*Corrected for decay from calibration date to measurement date.

†Measurement Set A, Table 1, minus background.

**TABLE III. CONVERSION FACTORS FOR EVALUATING SHALLOW (SKIN) DOSE EQUIVALENT FROM COUNT-RATE MEASUREMENTS: CASE B - SOURCE DISC CENTERED 1 CM FROM, AND PARALLEL TO, PROBE FACE.**

NUCLIDE	dpm	(cpm) <sub>o</sub> †	(cpm)'‡	$\frac{(\text{cpm})'}{\text{dpm}}$	$V \left( \frac{\text{rem/h}}{\mu\text{Ci/cm}^2} \right)$	CF $\left( \frac{\text{rem/h}}{\text{cpm}} \right)$
<sup>99</sup> Tc	1.49x10 <sup>4</sup>	1942	2053	0.138	3.49	1.14x10 <sup>-5</sup>
<sup>90</sup> Sr/ <sup>90</sup> Y	6.46x10 <sup>4</sup> *	20299	24580	0.380	6.76/9.29	1.90x10 <sup>-5</sup>
<sup>14</sup> C	7.77x10 <sup>5</sup>	5986	7248	0.00933	1.09	5.62x10 <sup>-5</sup>
<sup>36</sup> Cl	1.78x10 <sup>5</sup>	28197	34144	0.192	7.44	1.75x10 <sup>-5</sup>
<sup>147</sup> Pm	3.81x10 <sup>5</sup> *	9758	11816	0.0310	2.19	3.18x10 <sup>-5</sup>

\*Corrected for decay from calibration date to measurement date.

†Measurement Set B, Table I, minus background.

‡Converted by geometrical factors from disc of radius  $r_o$  to 1 cm<sup>2</sup> area using  $(\text{cpm})' = (\text{cpm})_o G(0.564, 2.22)/G(r_o, 2.22)$

TABLE IV. CONVERSION FACTORS FOR EVALUATING SHALLOW (SKIN) DOSE EQUIVALENT FROM COUNT-RATE MEASUREMENTS: CASE C - SOURCE DISC CENTERED ON 1 CM<sup>2</sup> CYLINDRICAL COLLIMATOR, 1 CM FROM PROBE FACE.

NUCLIDE	dpm	(dpm/cm <sup>2</sup> )†	(cpm/cm <sup>2</sup> )‡	$\frac{\text{cpm}}{\text{dpm}}$	V ( $\frac{\text{rem/h}}{\mu\text{Ci/cm}^2}$ )	CF ( $\frac{\text{rem/h}}{\text{cpm}}$ )
<sup>99</sup> Tc	1.49x10 <sup>4</sup> \	2.94x10 <sup>3</sup>	183	0.0622	3.49	2.53x10 <sup>-5</sup>
<sup>90</sup> Sr/ <sup>90</sup> Y	6.46x10 <sup>4</sup> *	5.14x10 <sup>3</sup>	958	0.186	6.76/9.29	3.89x10 <sup>-5</sup>
<sup>14</sup> C	7.77x10 <sup>5</sup>	6.18x10 <sup>4</sup>	254	0.00411	1.09	1.19x10 <sup>-4</sup>
<sup>36</sup> Cl	1.78x10 <sup>5</sup>	1.42x10 <sup>4</sup>	1286	0.0906	7.44	3.70x10 <sup>-5</sup>
<sup>147</sup> Pm	3.81x10 <sup>5</sup> *	3.03x10 <sup>4</sup>	394	0.0130	2.19	7.59x10 <sup>-5</sup>

\*Corrected for decay from calibration date to measurement date.

†dpm/(active area of disc in cm<sup>2</sup>).

‡Measurement Set C, Table I, minus background.

APPENDIX A

EFFECTS OF THE TISSUE—AIR INTERFACE IN  
CALCULATIONS OF BETA—PARTICLE SKIN DOSE  
AT A DEPTH OF 70  $\mu\text{m}$



## APPENDIX A

**Effects of the Tissue-Air Interface in  
Calculations of Beta-Particle Skin Dose  
at a Depth of 70  $\mu\text{m}$ \***

Oakley H. Crawford, J. E. Turner, R. N. Hamm, and J. C. Ashley  
Health and Safety Research Division, Oak Ridge National Laboratory  
Oak Ridge, Tennessee 37831-6123, USA

## INTRODUCTION

The determination of the dose or dose equivalent at a depth of 70  $\mu\text{m}$  in skin (basal layer) from beta emitters on the surface represents a formidable technical problem. Since this quantity is not amenable to direct measurement, it has to be inferred from calculations. Because of the physical discontinuity of the skin-air interface and the tortuous paths that electrons follow, analytic calculations of beta-particle depth-dose curves are not feasible, even for uniformly contaminated skin. On the other hand, such conditions can, in principle, be handled by Monte Carlo procedures. A Monte Carlo code that treats in detail the transport and interactions of a primary electron and all of the secondary electrons it generates in soft tissue can be used to make the needed calculations. For given conditions of source and target geometry, one calculates a sufficient number of randomly generated beta-particle histories to provide the desired information within statistically acceptable fluctuations.

---

\*Research sponsored by the Office of Health and Environmental Research, U.S. Department of Energy, under contract DE-AC05-84OR21400 with Martin Marietta Energy Systems, Inc.

In the field of beta dosimetry, the Monte Carlo code developed by Berger (1963) has received the most widespread use. For point sources of monoenergetic electrons in an infinite water medium, Berger (1973) calculated the average energy deposition as a function of distance in spherical shells surrounding the source using cross sections determined for electrons in water. (Results calculated for water and soft tissue are assumed to be the same.) The resulting point-source kernels for the infinite medium were subsequently used by Kocher and Eckerman (1987) to calculate dose-rate conversion factors for uniform skin contamination for a large number of beta-emitting nuclides. Kernels developed earlier by Berger (1971) are employed in the widely used computer code VARSKIN (Traub et al. 1987), which can be run on a personal computer.

Efforts have been made in the past to include the effects of the air-tissue interface on the depth-dose distribution in tissue. On the basis of a model Monte Carlo study, Berger (1970) has estimated the absorbed-dose reduction factor, which gives the decrease in the dose as compared with the dose in an unbounded medium. For planar isotropic sources, the reduction factor was found to be the same for all six radionuclides studied, within statistical errors, when the factor is expressed as a function of  $z/R_{\max}$ , where  $z$  is the depth and  $R_{\max}$  is the CSDA range of the maximum-energy beta particle. Henson (1972, 1973) calculated dose rates at various depths in water, for several radionuclides, using Berger's point-source kernels and reduction factor. More recently, Rohloff and Heinzelmann (1986) and Rohloff (1986) have used Monte Carlo methods to evaluate dose rates in tissue and water. Calculated dose-rate reduction factors were found to agree reasonably well with the earlier set (Berger 1970), although differences for the radiation from different nuclides were observed. In addition, these authors review the small number of earlier calculations on interface effects and

compare with experimental measurements of Osanov and Podsevalov (1971) using point sources and tissue-equivalent absorbers.

The purpose of this note is to assess the effect that the tissue-air interface at the skin surface has on the basal-layer dose at 70  $\mu\text{m}$  using a full, interaction-by-interaction, Monte-Carlo simulation to compare with the dose determined by using point-source kernels for an infinite tissue medium. Calculations are carried out with the Oak Ridge Electron-Transport Code, OREC (Turner et al. 1988).

### METHOD OF CALCULATION

OREC calculates the full Monte Carlo transport and energy loss of a primary electron and all of its secondaries in liquid water. For the present work, a new version of the code is used, which incorporates an air-water interface and uses improved values of cross sections for elastic scattering of electrons from H and O atoms. Inverse mean free paths for electrons in air are assumed to be the same as in water, except for scaling by the ratio of densities. In order to reduce statistical fluctuations in the determination of the interface effect, Monte Carlo histories are generated for beta particles in the all-water system and in the air-water system by using the same random-number sequence for both.

Differential elastic cross sections tabulated by Riley et al. (1975) and by Berger (1989) are used for electron energies from 10 keV to 256 keV and above 256 keV, respectively, for scattering from H and O atoms. (In the present calculations, electrons of energy less than 10 keV are assumed to deposit their remaining energy locally, without further transport.) These cross sections resulted from Riley's code (Riley 1974), which solves the Dirac equation for scattering of an electron in a static, central potential field, the latter being given by

electron-density distributions obtained from Hartree-Fock (Riley et al. 1975) or relativistic Hartree-Fock (Berger 1989) calculations for the atoms.

The method of interpolation is important, because cross sections are given in the above tabulations at energies of  $2^n$  keV (integer  $n$ ) only. Between any adjacent pair of these energies, we assume that the ratio of the differential cross section to a selected fitting function varies linearly with energy, for a fixed value of  $p\sin(\theta/2)$ ,  $p$  being the momentum of the electron and  $\theta$  its scattering angle in the laboratory frame. Various approximate expressions for relativistic electron scattering from Coulomb (or screened Coulomb) potentials are used as fitting functions in different ranges of energy and  $p\sin(\theta/2)$ , using in each range the approximation that gives the best fit.

### POINT SOURCES

Figure 1 shows the geometry used for calculations of the dose at a depth of 70  $\mu\text{m}$  from a 1-Bq source located at a point S on the surface of the water. The energy absorbed in the water layer between 65  $\mu\text{m}$  and 75  $\mu\text{m}$ , used to represent the basal layer at 70  $\mu\text{m}$ , is calculated in concentric rings about an axis passing perpendicularly through the water surface at S. From these data, the absorbed dose rate at the depth of 70  $\mu\text{m}$  per Bq of source strength can be calculated as a function of  $r$ , the distance from the axis. For beta particles emitted from S that stay entirely in the water, the presence of the air above, rather than the water, makes no difference in the energy they deposit at 70  $\mu\text{m}$ . However, the discontinuity makes a big difference for beta particles that are emitted into the air from S or that are backscattered from the water into the air before later reaching the layer at 70  $\mu\text{m}$ . An electron with the path (1) in the Air/H<sub>2</sub>O geometry in Fig. 1 would have the path (1') if water were present above the surface (H<sub>2</sub>O/H<sub>2</sub>O). [The situation is akin to a reverse "wall

effect," familiar with gas proportional counters used in microdosimetry (ICRU 1983).] The effect of the air is to spread the energy deposition in the basal layer to larger distances from the source. Therefore, the Air/H<sub>2</sub>O dose rate starts out smaller than the H<sub>2</sub>O/H<sub>2</sub>O dose rate at small  $r$ , but exceeds it at large  $r$ . In addition, the energy deposited in the basal layer is identical for paths 1 and 1' because of the proportionality of the air and water inverse mean free paths and use of the same sequence of random numbers.

As an example, we show results for a 1-Bq source of <sup>36</sup>Cl at S. The maximum beta-particle energy is 714 keV. We let  $\dot{D}(r)$  represent the absorbed dose rate per unit activity at 70  $\mu\text{m}$  as a function of the lateral distance  $r$  from a point below S. Figure 2 shows a plot of  $r^2\dot{D}(r)$  as a function of  $\log_{10}r$  for the Air/H<sub>2</sub>O and H<sub>2</sub>O/H<sub>2</sub>O cases. Using the weighting factor  $r^2$  and plotting  $r^2\dot{D}(r)$  makes the areas under the curves in Fig. 2 between, say,  $\log r_1$  and  $\log r_2$  proportional to the rate at which energy is deposited between  $r_1$  and  $r_2$  in the basal layer per beta particle emitted per unit time. The OREC curves have been smoothed in order to eliminate the statistical fluctuations in the raw Monte Carlo results.

The most striking aspect of Fig. 2 is the occurrence of two widely separated maxima in the Air/H<sub>2</sub>O curve. These two peaks, one at 0.01 cm and the other at about 20 cm, are attributable, respectively, to two classes of electrons: those that remain in water and those that travel through air before entering (or re-entering) water. An electron in air travels 844 times farther than one in water before making another collision. One also sees from the figure that the second peak is entirely absent from the H<sub>2</sub>O/H<sub>2</sub>O curve, and that the H<sub>2</sub>O/H<sub>2</sub>O values of  $\dot{D}$  are larger than the Air/H<sub>2</sub>O values at small  $r$ . The total areas under the Air/H<sub>2</sub>O and H<sub>2</sub>O/H<sub>2</sub>O curves are equal, due to the equality of the total energy deposition, mentioned above.

The chained curve in Fig. 2 gives results obtained with the VARSKIN code (Traub et al. 1987). This program calculates dose (or dose equivalent) in the basal layer, starting with point-source kernels for beta emitters immersed in an infinite water medium (Berger 1971). One sees that VARSKIN gives results similar to OREC for the infinite water medium ( $\text{H}_2\text{O}/\text{H}_2\text{O}$ ). This finding is not surprising, since neither treatment includes an interface.

Results for a  $^{14}\text{C}$  point source are shown in Fig. 3. The maximum and average beta-particle energies are 156 keV and 45 keV. As compared with Fig. 2, the curves are shifted to smaller  $r$ , and the differences between the Air/ $\text{H}_2\text{O}$  and  $\text{H}_2\text{O}/\text{H}_2\text{O}$  curves are not as large. Both effects are due to the smaller energies of the  $^{14}\text{C}$  beta rays and their resultant shorter ranges compared with  $^{36}\text{Cl}$ . The smaller relative difference between the  $^{14}\text{C}$  curves, with and without the interface occurs because, in order to contribute to the basal-layer dose, a beta ray that has traveled in air must still enter the tissue and penetrate to a depth of 70  $\mu\text{m}$ . Relative fewer of the lower-energy  $^{14}\text{C}$  beta particles do this, and so the presence or absence of an interface is less important for  $^{14}\text{C}$  than for  $^{36}\text{Cl}$ .

### DISTRIBUTED SOURCES

Figure 4 illustrates the geometry and coordinate system used for distributed-source calculations. A 1-Bq source is assumed to be distributed uniformly over a circular region of area  $A_S$  on the surface of the skin. One is often interested in the dose averaged over a circular target region directly below in the basal layer (70  $\mu\text{m}$  deep). The target area is assumed to be 1  $\text{cm}^2$ , the minimum usually of interest in skin dosimetry (ICRP 1977; NCRP 1989).

The dose rates, averaged over a 1  $\text{cm}^2$  region in the basal layer for a uniformly distributed source of  $^{36}\text{Cl}$ , are presented in Fig. 5 as functions of the source area  $A_S$ . These

values were obtained by convolution of the point-source results presented above. A constant activity of 1 Bq is assumed, regardless of the source area. One sees that the H<sub>2</sub>O/H<sub>2</sub>O and VARSKIN results are close together. However, they are respectively 46% and 38% above the Air/H<sub>2</sub>O results, for point sources and sources ranging up to 1 cm<sup>2</sup> in area. These findings are implicit in the discussion concerning Fig. 2. The measurements of Osanov and Podsevalov (1971) indicate an increase of ~30% when the absorber is polyethylene instead of water.

Because the basal layer lies so close to the skin surface compared with the radius of the target area, there is very little change in the dose rate as  $A_S$  increases from 0 to 1 cm<sup>2</sup>, the size of the target area. Thereafter, for  $A_S > 1$  cm<sup>2</sup>, the dose rates in the target decrease essentially as the inverse of the activity density, i.e., as  $A_S^{-1}$ . At the same time, the ratio of the H<sub>2</sub>O/H<sub>2</sub>O and Air/H<sub>2</sub>O results approaches unity.

Figure 6 presents the same kind of information for a distributed source of <sup>14</sup>C as given in Fig. 5 for <sup>36</sup>Cl. In this case, with the lower-energy beta particles, the results from the H<sub>2</sub>O/H<sub>2</sub>O and the VARSKIN calculations agree to 2% and exceed those from the Air/H<sub>2</sub>O calculation by about 10% for  $A_S < 1$  cm<sup>2</sup>. An increase of ~8% is found for a polyethylene absorber (Osanov and Podsevalov 1971).

From Fig. 6 for a point source ( $A_S \rightarrow 0$ ), the dose rate averaged over 1 cm<sup>2</sup> at a depth of 70 μm is ~0.26 μGy/h. For comparison, Henson's (1973) calculations yield a slightly larger value of 0.28 μGy/h for <sup>14</sup>C, while Rohloff and Heinzelmann (1986) predict an even higher value of ~0.33 μGy/h for their unit density "tissue" medium. Additional calculations for other radioisotopes should be made to isolate the source of these differences.

The ratio of Air/H<sub>2</sub>O and H<sub>2</sub>O/H<sub>2</sub>O dose rates in the basal layer, at a point centered below a planar source, may be compared with values of the absorbed-dose reduction factor

calculated according to Berger's (1970) prescription. These dose rates, from a 1-Bq, 1-cm<sup>2</sup> planar source, are related to quantities calculated here by a well-known symmetry principle. Their values are given directly by the intercepts of the curves with the left-hand vertical axes of Figures 5 and 6. For <sup>36</sup>Cl, the ratio of the calculated dose rates is  $0.68 \pm 0.02$ , while Berger's method (1970) for the reduction factor gives 0.76. For <sup>14</sup>C, the corresponding quantities are  $0.90 \pm 0.02$  and 0.94, respectively. (The error estimates are  $\pm 2\sigma$ , where  $\sigma$  is the standard deviation of the corresponding Monte Carlo result.) The agreement is reasonably good. It is interesting to note that for both nuclides the ratio of computed dose rates is less than the reduction factor estimated from Berger's prescription (1970), although the latter is supposed to give a lower bound for the ratio.

### SUMMARY

We find that dose rates at a depth of 70  $\mu\text{m}$  calculated by OREC and by VARSKIN for point and extended beta sources on the skin surface are in reasonable agreement when the air-tissue interface is ignored. However, dose rates calculated for air/tissue systems differ from corresponding infinite-tissue values. The differences are due to beta particles that are emitted into the air (or that escape into air from tissue) and subsequently enter the skin and deposit energy in the basal layer. These beta particles tend to deposit their energies at much greater lateral distances in the air/tissue system than in the infinite tissue medium. Thus, neglect of the interface leads to an overestimate of the dose rate in regions below a small-area source; differences are greater for beta sources of higher energy. Furthermore, the

differences are somewhat greater than predicted by Berger's estimate (1970) of the dose-rate reduction factor.

While neglect of the air-tissue interface appears to be on the conservative side for beta-particle skin dosimetry, its effects should be thoroughly understood and evaluated. Further studies are needed to carry out this task.

*Acknowledgments*--The authors thank Dr. Martin J. Berger for providing values of differential elastic cross sections. They also thank Dr. Keith F. Eckerman for providing the energy spectra used for  $^{36}\text{Cl}$  and  $^{14}\text{C}$ .

## REFERENCES

- Berger, M. J. Monte Carlo calculation of the penetration and diffusion of fast charged particles. *Methods Comput. Phys.* 1:135-215; 1963.
- Berger, M. J. Beta-ray dosimetry calculations with the use of point kernels. In *Medical Radionuclides: Radiation Dose and Effects*, eds. R. J. Cloutier, C. L. Edwards, and W. S. Snyder, CONF 691212 (Available from NTIS, Springfield, VA) pp. 63-86; 1970.
- Berger, M. J. Distribution of absorbed dose around point sources of electrons and beta particles in water and other media. (MIRD Pamphlet No. 7, Suppl. No. 5). *J. Nucl. Med.* 12:5-23; 1971.
- Berger, M. J. Improved point kernels for electron and beta-ray dosimetry. Washington, D.C.; National Bureau of Standards Rep. NBSIR 73-107; 1973.
- Berger, M. J. Private communication. 1989.
- Henson, P. W. A note on some aspects of skin contamination by certain radionuclides in common use. *Br. J. Radiol.* 45:938-943; 1972.
- Henson, P. W. Skin contamination: dose rates at reduced depth of basal layer. *Br. J. Radiol.* 46:645-646; 1973.
- ICRP Publication 26, Recommendations of the ICRP. International Commission on Radiological Protection, Pergamon Press, Elmsford, NY; 1977.
- ICRU Report 36, Microdosimetry. International Commission on Radiation Units and Measurements, Bethesda, MD, pp. 28-31; 1983.

- Kocher, D. C.; Eckerman, K. F. Electron dose-rate conversion factors for external exposure of the skin from uniformly deposited activity on the body surface. *Health Phys.* 53:135-141; 1987.
- NCRP Report No. 106, Limit for Exposure to "Hot Particles" on the Skin. National Council on Radiation Protection and Measurements, Bethesda, MD; 1989.
- Osanov, D. P.; Podsevalov, Yu. N. Dose function for a plane infinite thin source at the boundary of two media. *Sov. J. At. En.* 31:1025-1027; 1971.
- Riley, M. E. Relativistic, elastic electron scattering from atoms at energies greater than 1 keV. SLA-74-0107, Sandia Laboratories, Albuquerque, NM; 1974.
- Riley, M. E.; MacCullum, C. J.; Biggs, F. Theoretical electron-atom elastic scattering cross sections: selected elements, 1 keV to 256 keV. *Atomic Data and Nuclear Data Tables* 15:443-476; 1975.
- Rohloff, F.; Heinzelmann, M. Calculation of dose rates for skin contamination by beta radiation. *Radiat. Prot. Dosim.* 14:279-287; 1986.
- Rohloff, F. Beta transport calculation for beta dosimetry. *Radiat. Prot. Dosim.* 14:161-168; 1986.
- Traub, R. J.; Reece, R. I.; Scherpelz, R. I.; Sigalla, L. A. Dose calculations for contamination of the skin using the computer code VARSKIN. NUREG/CR-4418 (PNL-5610). Available from Radiation Shielding Information Center, Oak Ridge National Laboratory, Oak Ridge, TN; 1987.

Turner, J. E.; Hamm, R. N.; Souleyrette, M. L.; Martz, D. E.; Rhea, T. A.; Schmidt, D. W.  
Calculations for  $\beta$  dosimetry using Monte Carlo code (OREC) for electron transport  
in water. *Health Phys.* 55:741-750; 1988.

**FIGURE CAPTIONS**

1. Geometry for calculations (not to scale). A point source of unit activity is located at air/water interface at S. Dose rate in the layer between 65  $\mu\text{m}$  and 75  $\mu\text{m}$  is calculated as a function of the distance  $r$  from a perpendicular axis passing through S. The collision sites of an electron (1) that travels above the skin are compressed toward the axis (1') if the air above is replaced by water.

2. Dose rate of 70  $\mu\text{m}$  depth as a function of the radial distance  $r$  for a 1-Bq point source of  $^{36}\text{Cl}$  on the skin surface at S. The curves Air/ $\text{H}_2\text{O}$  and  $\text{H}_2\text{O}/\text{H}_2\text{O}$  were calculated with OREC for the air-water interface and for an infinite water medium, respectively. The raw results from the OREC calculations were averaged by a smoothing routine to obtain the curves shown. Results obtained by using VARSKIN, also shown, are virtually the same as those found with OREC for the infinite water medium ( $\text{H}_2\text{O}/\text{H}_2\text{O}$ ).

3. Dose rate at 70  $\mu\text{m}$  depth for 1-Bq point source of  $^{14}\text{C}$  on surface. Compared with  $^{36}\text{Cl}$  (Fig. 2), presence of interface has less effect on basal-layer dose from the lower-energy beta particles from  $^{14}\text{C}$ . As in Fig. 2, the raw results from the OREC calculations were averaged by a smoothing routine to obtain the curves shown.

4. Geometry and coordinates used to describe the dose rate, averaged over a  $1\text{-cm}^2$  circular area (the target) in the basal layer from a 1-Bq distributed source of beta particles directly above on the surface of the skin.

5. Dose rate averaged over a  $1\text{-cm}^2$  circle in the basal layer (70  $\mu\text{m}$  deep) of skin. A 1-Bq,  $^{36}\text{Cl}$  source is assumed to be distributed uniformly over a circular area  $A_S$  directly above. The dose rate is shown as a function of the area  $A_S$  covered by the source on the skin.

6. Dose rate averaged over a  $1\text{-cm}^2$  circle in the basal layer ( $70\ \mu\text{m}$  deep) of skin. A  $1\text{-Bq}$ ,  $^{14}\text{C}$  source is distributed uniformly over a circular area  $A_S$  directly above, on the surface of the skin.

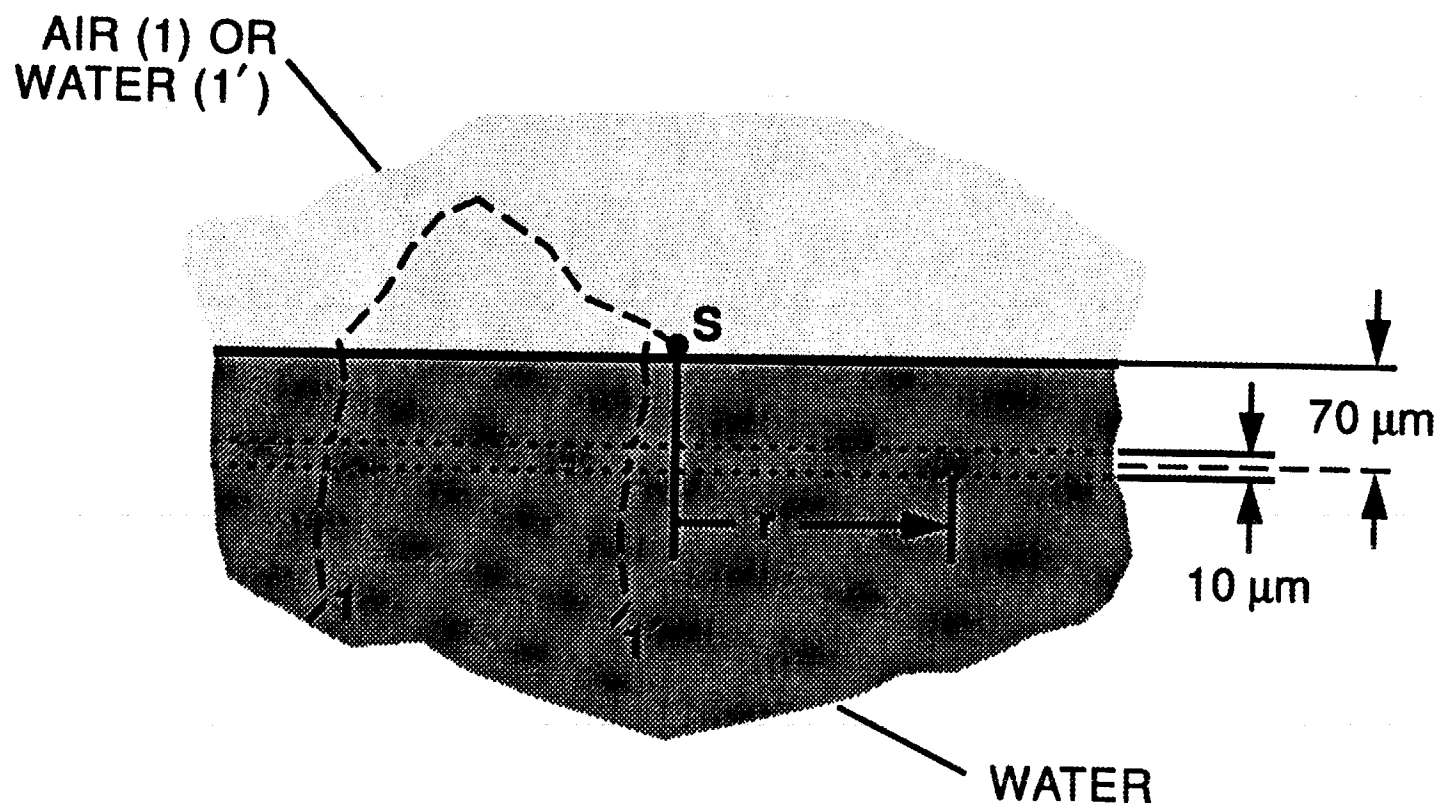


Fig. 1

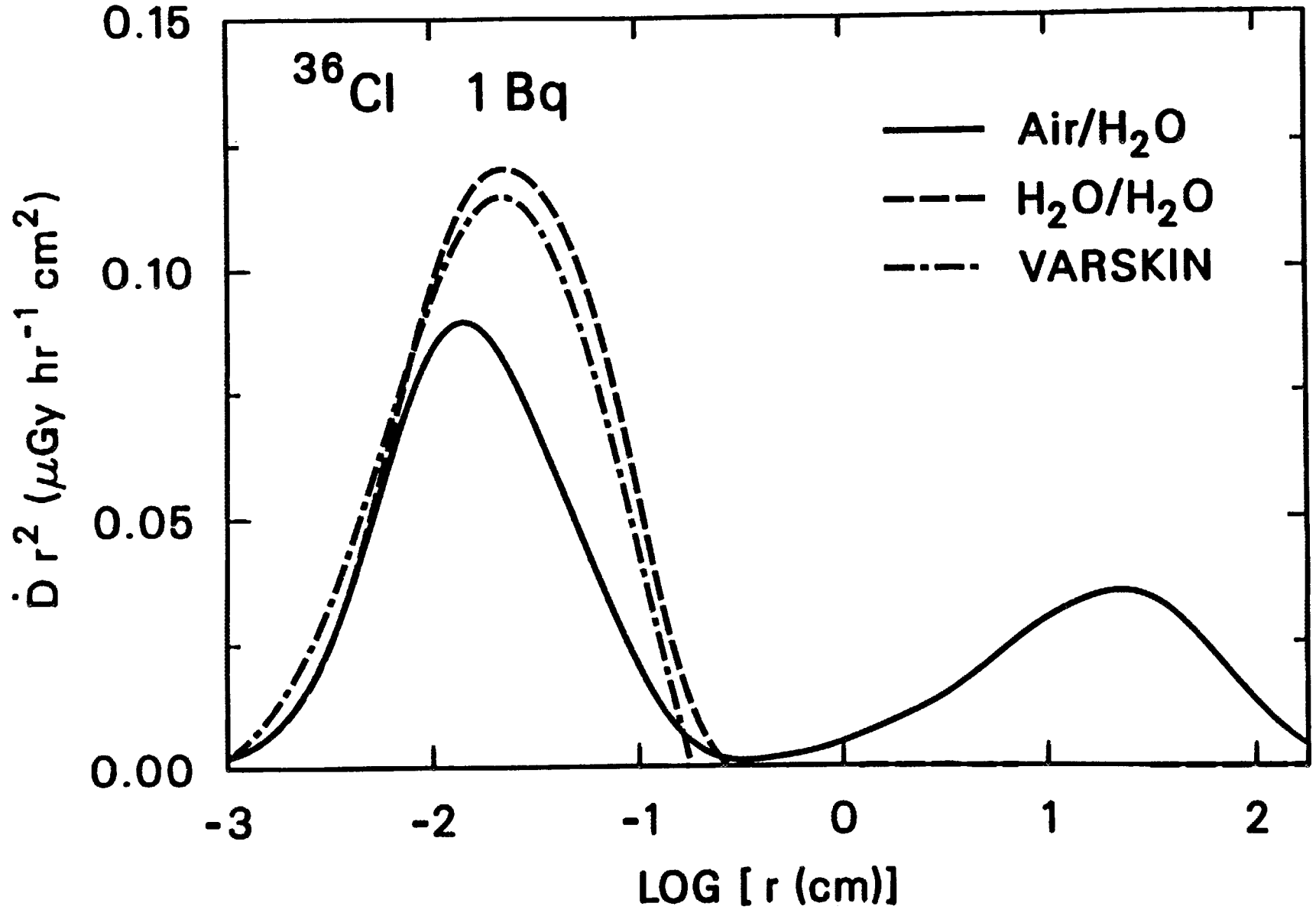


Fig. 2  
32

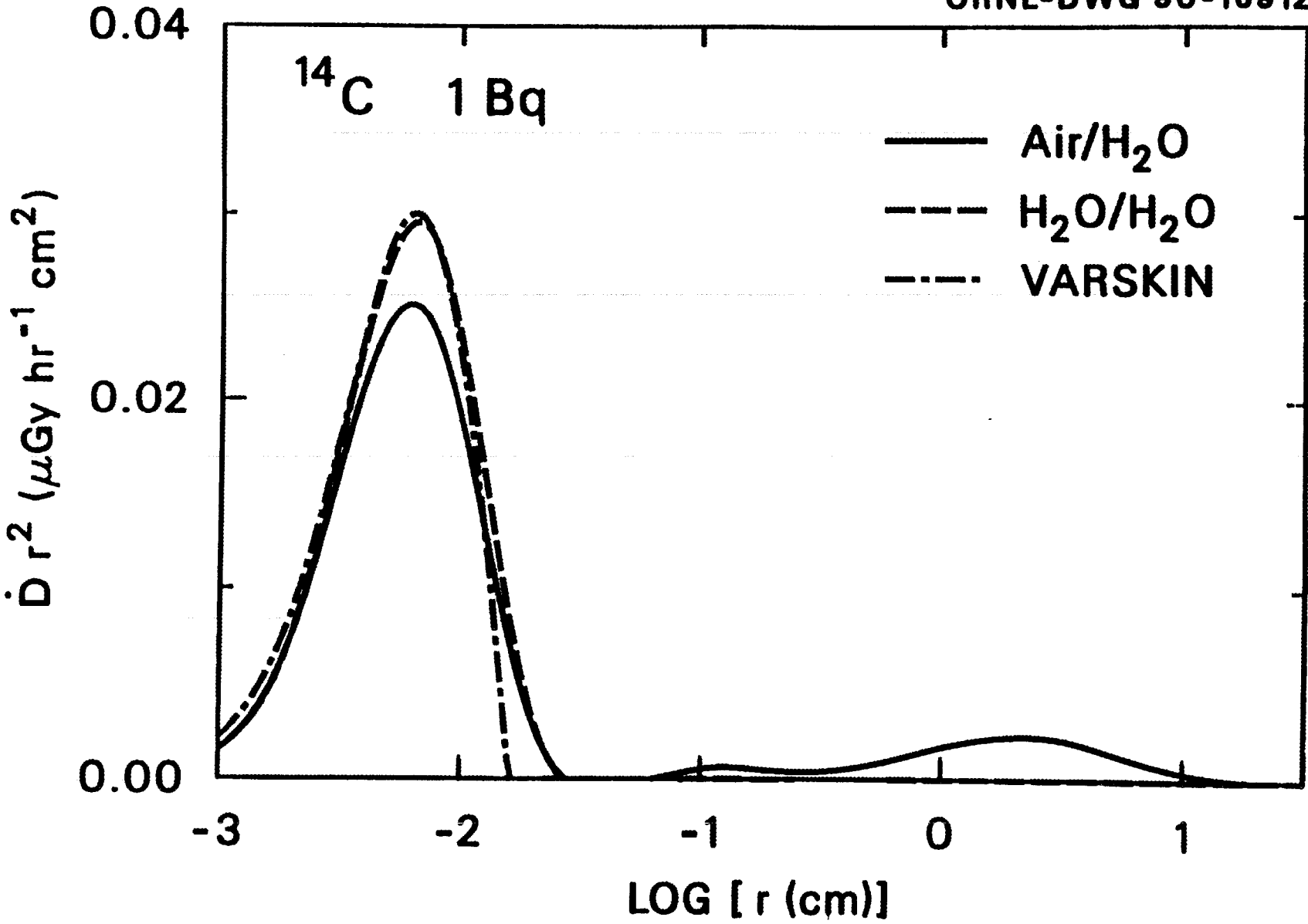


Fig. 3

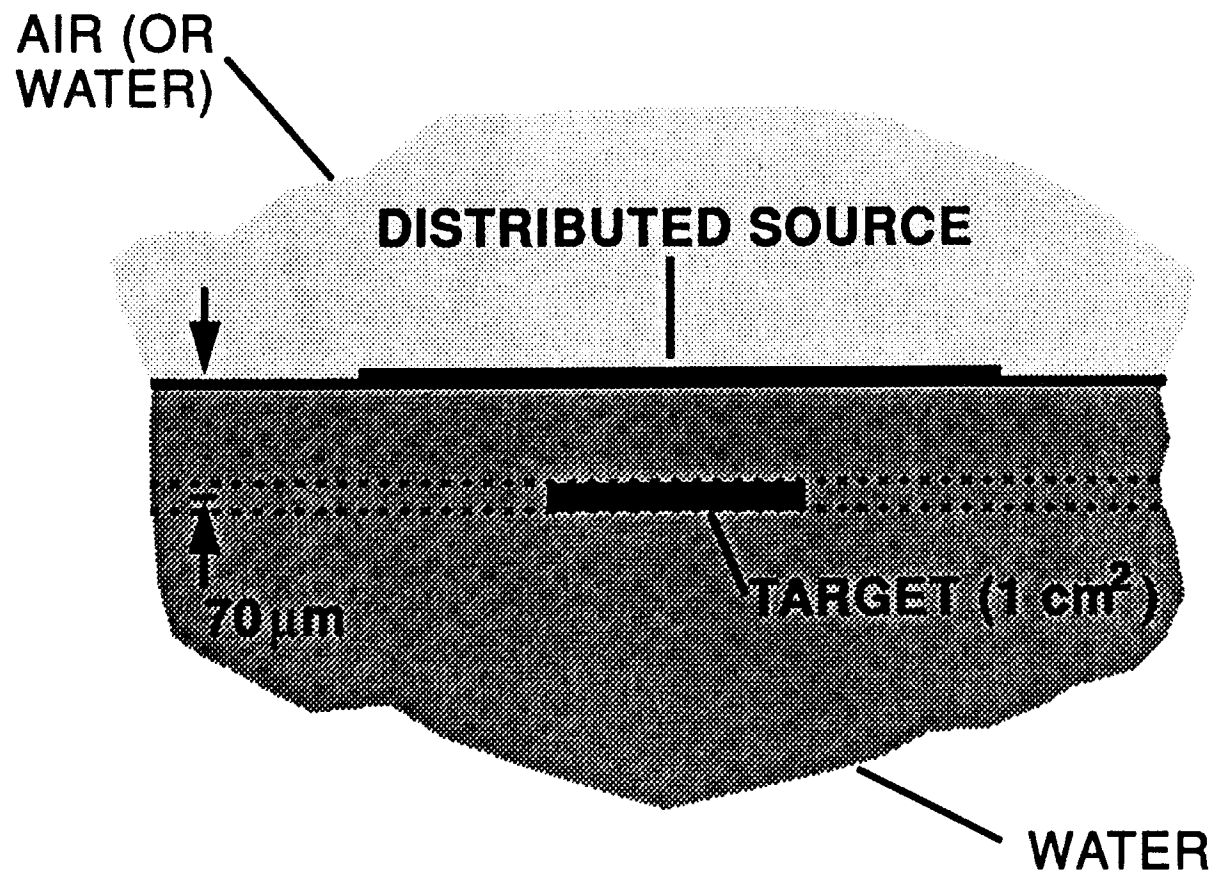
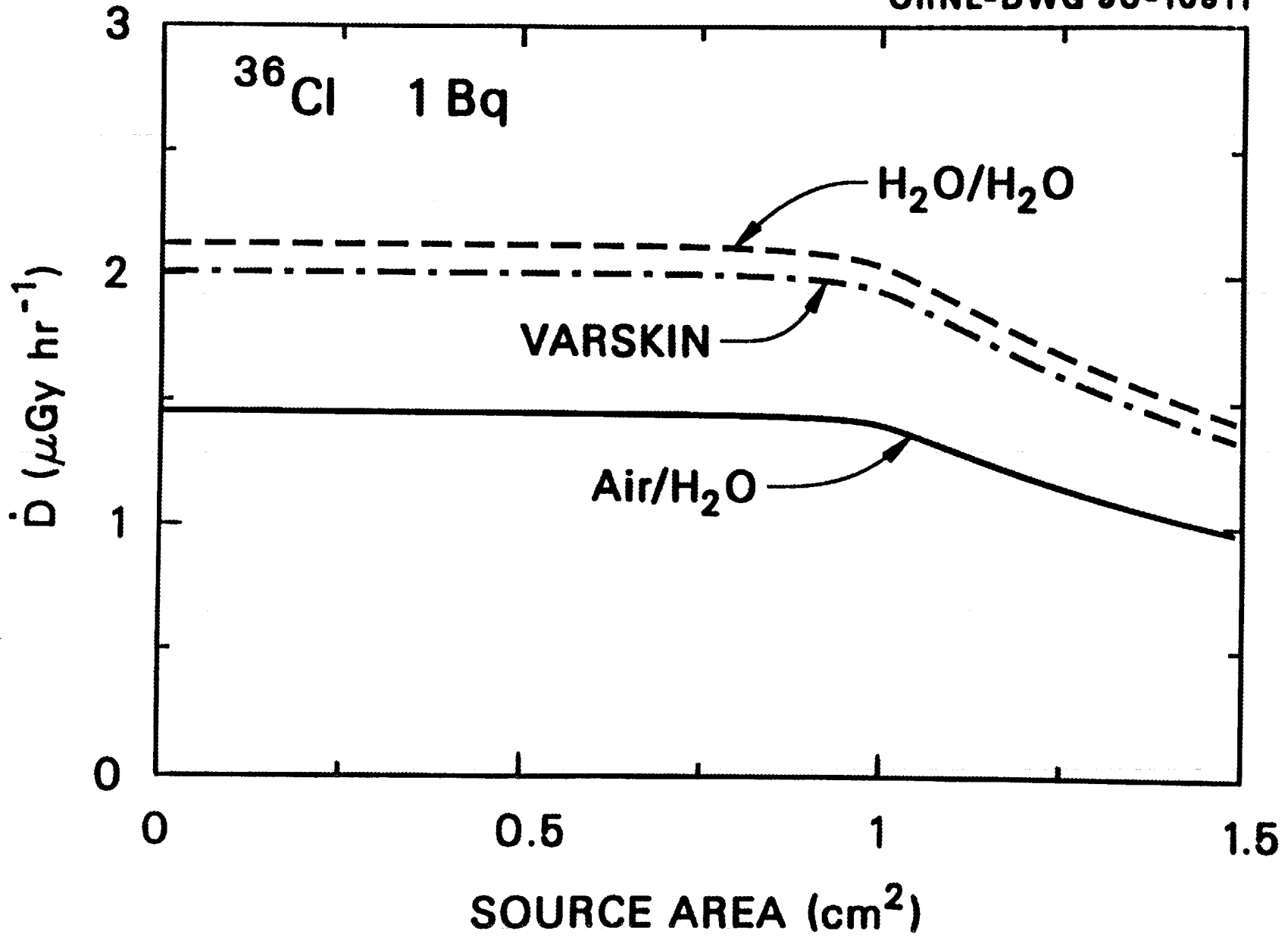


Fig. 4



35  
FIG. 5

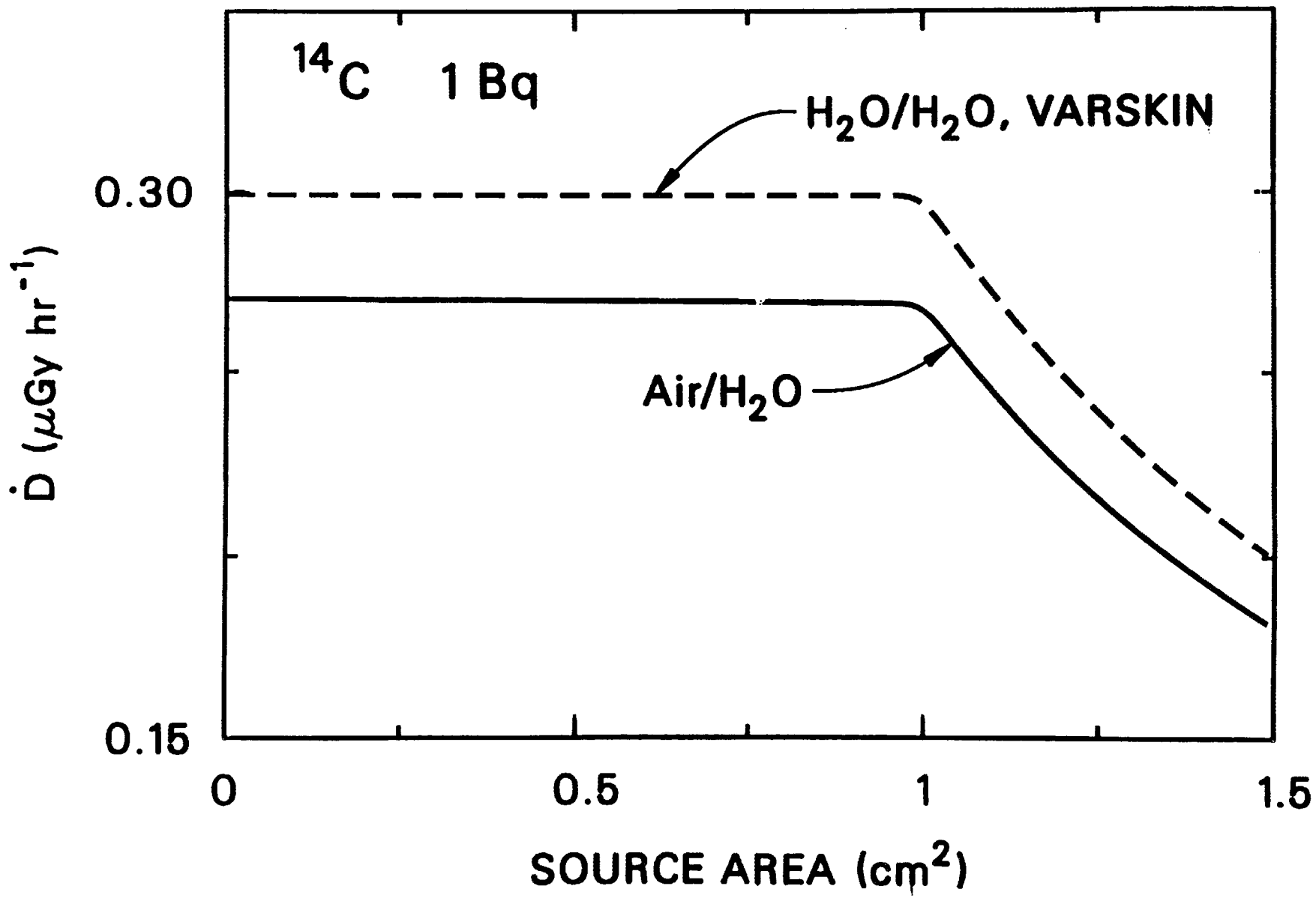


Fig. 6  
36

APPENDIX B  
SOLID-ANGLE (GEOMETRICAL) FACTORS

### Appendix B. Solid–Angle (Geometrical) Factors

When a beta source is surveyed with a probe that is held away from the source, the count rate is determined in part by the geometry factor,  $G$ , which may be defined as

$$G = \frac{1}{4\pi A_S} \int d^2r \Omega(\vec{r}),$$

where  $\Omega(\vec{r})$  is the solid angle subtended by the detector, at point  $\vec{r}$  on the source, and  $A_S$  is the area of the source. The integral extends over the surface of the source. Thus, the geometry factor is the average, over the source, of the solid angle subtended by the detector, all divided by  $4\pi$ . If we neglect scattering and self absorption in the source and the ambient air, then the fraction of emitted beta particles that enters the detector is given by  $G$ .

If the source and the detector are circular regions of radius  $r_S$  and  $r_D$ , respectively, and the detector is centered over the source, at distance  $a$ , the above expression becomes

$$G = \frac{1}{2\pi r_S^2} \int_0^{r_S} dr r \Omega(r),$$

with  $\Omega$  given by

$$\Omega(r) = \begin{cases} 2\pi \left[ 1 - \frac{a}{\sqrt{r_D^2 - r^2 + a^2}} \right] + 2a \int_{r_D - r}^{r_D + r} \frac{v}{(v^2 + a^2)^{3/2}} \cos^{-1} \left[ \frac{r^2 + v^2 - r_D^2}{2rv} \right], & r < r_D \\ 2a \int_{r - r_D}^{r + r_D} \frac{v}{(v^2 + a^2)^{3/2}} \cos^{-1} \left[ \frac{r^2 + v^2 - r_D^2}{2rv} \right], & r \geq r_D \end{cases}$$

Values of G for some geometries of interest in the skin-dose problem were computed from the above expressions, and are given in the table below. In each case  $a = 1$  cm. Note that the maximum possible value of G for this configuration is  $1/2$ .

TABLE – Geometrical Factors for Various Source and Detector Radii

Source radius $r_S$ (cm)	Detector radius $r_D$	$G(r_S, r_D)$
0	2.22	0.2946
0.564	2.22	0.2911
1.27	2.22	0.2754
2.00	2.22	0.2404
2.225	2.22	0.2253
0	0.564	0.0645
0.564	0.564	0.0560



## INTERNAL DISTRIBUTION

1. A. B. Ahmed
- 2-11. J. C. Ashley
12. J. S. Bogard
13. R. S. Bogard
14. H. M. Butler, Jr.
- 15-19. O. H. Crawford
20. S. W. Croslin
21. T. C. Dodd
- 22-26. R. N. Hamm
27. M. D. Henderson
- 28-30. J. B. Hunt
31. A. H. Jefferies
32. C. E. Maples
- 33-37. K. L. McMahan
38. G. T.-Y. Mei
39. G. L. Murphy
40. C. L. Pugh
- 40-44. K. L. Reaves
45. B. C. Thorpe
- 46-55. J. E. Turner
56. Central Research Library
57. ORNL Y-12 Technical Library
58. Document Reference Section
59. Laboratory Records
60. Laboratory Records-RC
61. ORNL Patent Section

## EXTERNAL DISTRIBUTION

62. Office of Assistant Manager for Energy Research and Development, Department of Energy, Oak Ridge Operations Office, Oak Ridge, TN 37831
63. M. N. Varma, Office of Health and Environmental Research, ER-70, U.S. Department of Energy, Washington, DC 20585
64. D. J. Galas, Office of Health and Environmental Research, ER-70, U.S. Department of Energy, Washington, DC 20585
65. R. W. Wood, Office of Health and Environmental Research, ER-70, U.S. Department of Energy, Washington, DC 20585
- 66-75. Office of Scientific and Technical Information, Oak Ridge, TN 37831